PL-TR-94-2198

PRISM VALIDATION

Robert E. Daniell, Jr.
William G. Whartenby
Lincoln D. Brown

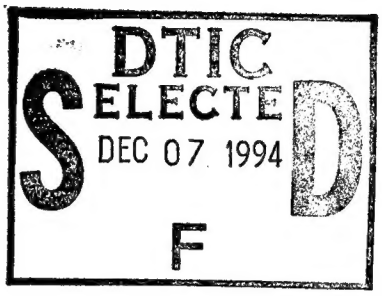

Computational Physics, Inc.
Suite 202A
240 Bear Hill Road
Waltham, MA 02154

13 June 1994

Scientific Report No. 1

PHILLIPS LABORATORY
Directorate of Geophysics
AIR FORCE MATERIEL COMMAND
HANSCOM AIR FORCE BASE, MA 01731-3010

"This technical report has been reviewed and is approved for publication"

Signature
CHRISTOPHER SHERMAN
Contract Manager

Signature
DAVID ANDERSON
Branch Chief

Signature
WILLIAM K. VICKERY
Division Director

This report has been reviewed by the ESC Public Affairs Office (PA) and is releasable to the National Technical Information Service (NTIS).

Qualified requestors may obtain additional copies from the Defense Technical Information Center (DTIC). All others should apply to the National Technical Information Service (NTIS).

If your address has changed, if you wish to be removed from the mailing list, or if the addressee is no longer employed by your organization, please notify PL/TSI, 29 Randolph Road, Hanscom AFB, MA 01731-3010. This will assist us in maintaining a current mailing list.

Do not return copies of this report unless contractual obligation or notices on a specific document requires that it be returned.

REPORT DOCUMENTATION PAGE

Form Approved
OMB No. 0704-0188

1. AGENCY USE ONLY (Leave blank)	2. REPORT DATE	3. REPORT TYPE AND DATES COVERED
	13 June 1994	Scientific Report No. 1

4. TITLE AND SUBTITLE

PRISM Validation

5. FUNDING NUMBERS

PE63707F
PR 4026 TA01 WULA

Contract F19628-92-C-0044

6. AUTHOR(S)

Robert E. Daniell, Jr., William G. Whartenby, & Lincoln D. Brown

7. PERFORMING ORGANIZATION NAME(S) AND ADDRESS(ES)

Computational Physics, Inc.
Suite 202A
240 Bear Hill Road
Waltham, MA 02154

8. PERFORMING ORGANIZATION REPORT NUMBER

9. SPONSORING / MONITORING AGENCY NAME(S) AND ADDRESS(ES)

Phillips Laboratory
29 Randolph Street
Hanscom AFB, MA 01731-3010
Contract Manager: Christopher Sherman/GPIM

10. SPONSORING / MONITORING AGENCY REPORT NUMBER

PL-TR-94-2198

11. SUPPLEMENTARY NOTES

12a. DISTRIBUTION / AVAILABILITY STATEMENT

APPROVED FOR PUBLIC RELEASE;
DISTRIBUTION UNLIMITED

12b. DISTRIBUTION CODE

13. ABSTRACT *(Maximum 200 words)*

This report describes the validation of PRISM, a parameterized, real-time ionospheric specification model, which was described in PL-TR-91-2299. Data were obtained from both analog and digital ionosondes, polarimeters measuring TEC, incoherent scatter radar (ISR), and *in situ* measurements of electron density, ion velocity, and auroral particle precipitation. Some of the data was used to "drive" the model while the remainder of the data was held in reserve for comparison with model output. We found that near ionospheric measurements (i.e., within the decorrelation length of the ionosphere), PRISM provides better than 50% improvement in f_oF_2, N_mF_2, and TEC over the ICED, the currently operational ionospheric model at AFSFC. At distances beyond the decorrelation length, PRISM performs as well as ICED and other climatological models. We conclude that PRISM will significantly enhance the ionospheric specification capability of AFSFC.

14. SUBJECT TERMS	15. NUMBER OF PAGES
ionosphere, space environment, space weather, ionospheric specification, model validation	46
	16. PRICE CODE

17. SECURITY CLASSIFICATION OF REPORT	18. SECURITY CLASSIFICATION OF THIS PAGE	19. SECURITY CLASSIFICATION OF ABSTRACT	20. LIMITATION OF ABSTRACT
Unclassified	Unclassified	Unclassified	SAR

Table of Contents

Executive Summary

The Parameterized Real-time Ionospheric Specification Model (PRISM) Version 1.2 has been validated against actual data for 6 days during October 1989, a period of high solar activity. The specific dates were chosen based on the availability of Incoherent Scatter Radar (ISR) and Digisonde data. The results are summarized in the following table.

Summary of PRISM and ICED validation results

Quantity	ICED	PRISM	Improvement
RMS f_oF_2 error (Mhz)	1.5 Mhz	0.7 Mhz	54%
RMS N_mF_2 error (%)	40%	20%	50%
RMS TEC error (TEC units)	7.1	3.1	56%
RMS TEC error (%)	31%	8%	74%
RMS h_mF_2 error (km)	25 km	6 km	75%

The "Improvement" column indicates the improvement in PRISM's specification of each ionospheric parameter over ICED's specification of the same parameter. It is defined as

$$\frac{\text{ICED RMS error - PRISM RMS error}}{\text{ICED RMS error}}$$

so that when PRISM's error is smaller than ICED's, the improvement is positive. A zero PRISM error results in the greatest possible improvement of 100%.

We have demonstrated that PRISM is capable of ingesting ionospheric data from both ground based and space based sources and of using that data to provide a significantly improved ionospheric specification compared to climatological models. PRISM is capable of ingesting and using data from new sources (such as UV imaging) that will become available during the next decade.

1. Introduction

The Parameterized Real-time Ionospheric Specification Model (PRISM) is a parameterization of several physically based ionospheric models with the capability of adjusting its ionospheric specification based on real-time (or near real-time) data from both ground based and space based sources. It is intended to replace the Ionospheric Conductivity and Electron Density (ICED) model as the primary ionospheric specification tool at the Air Force Space Forecast Center (AFSFC).

PRISM Version 1.0 was delivered to the Air Weather Service (AWS) early in 1992. This version of PRISM and the operational version of ICED were validated using data from October 1987, a period of low to moderate solar activity. That validation effort is described in a report dated 8 September 1992. Because PRISM performance, although superior to ICED's in several respects, was disappointing overall, a new real-time adjustment algorithm was developed. The old algorithm was based on least squares fitting of a ten parameter function of latitude and longitude. The new algorithm is based instead on a weighted mean that guarantees that PRISM's specification will match the data at the location at which the data was taken. This has the advantage that when customer support is provided for a location at which ionospheric data is available, PRISM will reproduce that data. The new algorithm was incorporated into PRISM 1.1, which was delivered to the Air Force Space Forecast Center (AFSFC) on 3 May 1993. PRISM 1.2, incorporating minor changes to the data ingestion and data handling algorithms was delivered on 4 June 1993.

Because ICED had never undergone a thorough validation, we were asked to run ICED using the same validation data set used for PRISM. We have done so, and the results are reported below for comparison to PRISM performance.

We acquired data from numerous sources for this effort. Although we acquired some data for several months during the most recent sunspot maximum, it quickly became apparent that the most complete data were those for October 1989. Therefore, we have concentrated exclusively on that period. Within that month, Incoherent Scatter Radar (ISR) data was available at multiple sites only on the days 2-6 October. It also turned out that Digisonde data (as opposed to data from analog ionosondes) was available primarily later in the month when ISR data is not available. So we added another day, 9 October, in order to make better use of the Digisonde data. Thus, the statistical results presented here generally apply to 6 days worth of data.

As we describe below, the difficulties of obtaining a complete set of historical data to validate an ionospheric model are substantial. Therefore, we feel quite strongly that further validation must be performed after PRISM has become operational. This will require that both data and PRISM output be archived on a regular basis for later analysis. PL/GPI and CPI will need to acquire data from other sources for these same time periods in order to assess PRISM performance and to identify problems that require correction. The periods for such archival and analysis should be agreed upon in advance (e.g., "World Days").

2. Data Acquisition

The minimum data set needed to run PRISM is the daily value of $F_{10.7}$ and the current value of K_p. $F_{10.7}$ is the solar flux at 10.7 cm (2800 MHz) in units of 10^{-22} W m^{-2} Hz^{-1}. PRISM can accept sunspot number, *SSN*, in lieu of $F_{10.7}$. The "official" values of $F_{10.7}$ and *SSN* are compiled and published by NGDC from observations made by designated solar observatories. K_p is a measure of geomagnetic activity calculated from magnetometer data. The "official" values are also compiled and published by NGDC for eight three hour periods each day. At AFSFC, a "pseudo-K_p" value will be calculated at more frequent intervals.

ICED requires the "effective sunspot number," SSN_{eff}, and the auroral Q index. SSN_{eff} is calculated from ionosonde data (see discussion in Section 3, below) as the *SSN* value which produces the best agreement (in a least squares sense) between f_oF_2 calculated from the URSI coefficients and the measured values. The auroral Q index is related to the midnight equatorward precipitation boundary, but it is calculated from K_p (see discussion in Section 3, below).

We obtained the daily values of $F_{10.7}$ and the three-hourly values of K_p from the *Solar Indices Bulletin* and *Geomagnetic Indices Bulletin* for October 1989. These bulletins are published by NGDC. The values we used are listed in Table 1.

Table 1. Daily $F_{10.7}$ and 3-hourly K_p for 2-6 and 9 October 1989.

	2	3	4	5	6	9
daily $F_{10.7}$	208.5	222.4	234.1	223.2	220.5	201.9
3-hrly K_p:						
00-03 UT	1+	1-	2	2+	2	3+
03-06 UT	4-	1	2	1	1	4-
06-09 UT	3-	2	1	0	2	2+
09-12 UT	2	3-	1-	1	3-	2-
12-15 UT	2	4-	2	2	3-	2
15-18 UT	2+	3+	2+	1	3	1+
18-21 UT	2-	4-	1	1	2+	2
21-24 UT	1	2+	2	2-	3	3

In addition to these global parameters, PRISM can accept real-time measurements of ionospheric parameters from a variety of sources, ground based and space based. Since we do

not have access to the Environmental Database at AFSFC, and since the full set of ionospheric measurements is not yet available, we had to acquire similar historical data from other sources.

1. *analog ionosondes:* critical frequencies (f_oF_2 and f_oE) hand scaled from analog ionograms from over 30 sites around the world; supplied by R. Conkrite of the National Geophysical Data Center (NGDC) and supplemented by some additional data from the Australian Ionospheric Prediction Service (IPS) obtained by M. Fox of Boston University.

2. *digital ionosondes:* critical frequencies and true height analysis from five Digisondes; supplied by B. Rheinisch and R. Gamache of the University of Massachusetts, Lowell.

3. *polarimeters:* total electron content (TEC) from four polarimeters; supplied by J. Klobuchar of PL/GPIM and P. Doherty of Boston College

4. *ISR data:* electron density profiles (EDP's) from four incoherent scatter radar facilities; supplied by R. Barnes of the National Center for Atmospheric Research (NCAR). (However, the data from one of the facilities, EISCAT, were obtained at 21.5° elevation angle and were not used in this validation effort.)

5. *in situ plasma data:* total ion density and one component of the horizontal ion drift as measured by the Scintillation Meter on the SSIES instrument package on the DMSP satellites F8 and F9. (Neither ion nor electron temperature was available from these flights for October 1989.) Software and other information for accessing the data tapes was supplied by F. Rich of PL/GPS.

6. *precipitating electron and ion data:* electron and ion fluxes measured by the SSJ/4 instrument on the DMSP satellites F8 and F9. Information for accessing the data tapes was supplied by F. Rich of PL/GPS.

The quality and quantity of the data from each of these sources along with the processing required to utilize the data for PRISM and ICED validation are described below.

2.1 *Analog Ionosondes*

The National Geophysical Data Center (NGDC) in Boulder, Colorado maintains an extensive database of historical ionospheric data. The October 1989 data was originally supplied on floppy disk, but we later obtained a pair of CD-ROM disks containing the entire database of ionosonde data from 1957 through 1991. However, a search of the CD-ROM revealed no data from October 1989 that had not been provided on the floppy disk.

Matthew Fox of Boston University contacted the Australian Ionospheric Prediction Service (IPS) and obtained f_oF_2 data from several Australian ionosondes for October 1989. Most of this data duplicated the NGDC data, but in one case (Mundaring, MU 43K) the NGDC data included only f_oE so the IPS f_oF_2 data was added to the database. The IPS data were reformatted into the NGDC format and added to the validation data.

A list of the combined NGDC and IPS stations is provided in Table 2. The two and three character station codes are those assigned by the World Data Center. A map of the station locations (along with the Digisonde, polarimeter, and ISR locations) is provided in Figure 1. It is obvious from the map that coverage is not uniform around the globe. The highest concentration of ionosondes is in Europe with a secondary cluster in and near Australia. Otherwise, much of the globe is either underrepresented or not represented at all. This is particularly true of the southern hemisphere and the equatorial region. Furthermore, not all stations had data at all times. Many stations had data for only part of each day while other stations had data for only some days during the month. So at any given UT on any given day, the ionosonde coverage is even more sparse than the map indicates.

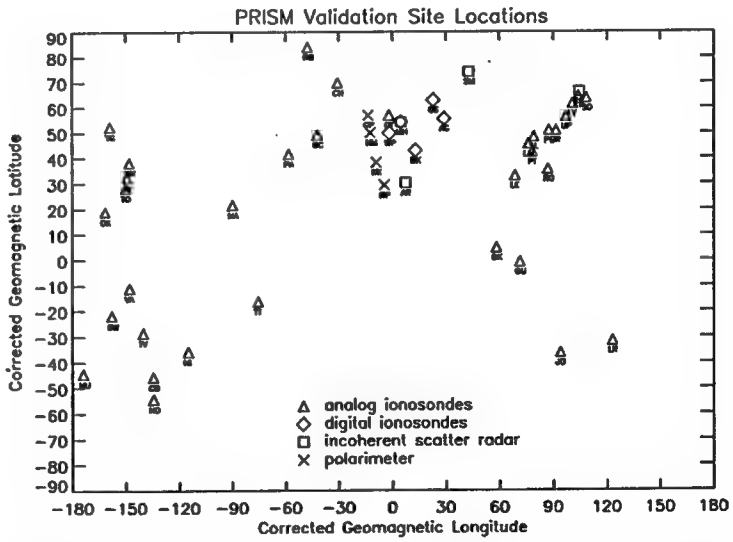

Figure 1. A map in geomagnetic coordinates of the locations of ionosondes, polarimeters, and incoherent scatter radars used for PRISM validation. Note that the polarimeter positions indicate the ionospheric intersection points rather than the ground sites.

The analog ionosonde data sets were surveyed for data availability during 2-6 October and on 9 October. The results are displayed in Figure 2 for both f_oF_2 and f_oE. Clearly, much more F region data is available than E region data. Consequently, most of our validation effort has concentrated on the F region data.

Some stations were very reliable, providing hourly f_oF_2 data 24 hours a day, or nearly so. Other stations operated only during a portion of each day, or only sporadically. However, whenever data is available, we believe it to be of high quality because it is carefully checked at

Table 2. Analog ionosonde sites supplied by NGDC and the Australian IPS.

geographic lat	geographic lon	magnetic lat	magnetic lon	Station codes	Station Name	Source
12.40	358.50	-0.89	71.32	OU 012	OUAGADOUGOU	NGDC
38.70	350.70	32.90	68.73	LE 038	LISBONNE	NGDC
41.80	12.50	35.57	87.11	RO 041	ROME	NGDC
46.60	0.30	42.23	78.32	PT 046	POITIERS	NGDC
48.80	356.60	45.43	76.07	LN 047	LANNION	NGDC
51.50	359.40	48.30	79.16	SL 051	SLOUGH	NGDC
54.30	8.60	50.77	87.51	PE 054	ST PETER-ORDING	NGDC
54.60	13.40	50.81	91.52	JR 055	JULIUSRUH/RUGEN	NGDC
-26.10	28.10	-36.30	93.95	JO 120	JOHANNESBURG	NGDC
59.80	17.60	56.26	97.02	UP 158	UPPSALA	NGDC
64.70	18.80	61.32	100.69	LY 164	LYCKSELE	NGDC
67.40	26.60	63.60	108.55	SO 166	SODANKYLA	NGDC
67.90	20.30	64.48	104.06	KI 167	KIRUNA	NGDC
-21.10	55.90	-31.53	123.19	LR 22J	LA REUNION	NGDC
-12.40	130.90	-21.93	202.26	DW 41K	DARWIN	NGDC
26.30	127.80	18.93	198.56	OK 426	OKINAWA	NGDC
58.80	130.60	52.38	201.20	YG 431	YAMAGAWA	NGDC
-32.00	116.20	-44.61	186.18	MU 43K	MUNDARING	NGDC & IPS
-2.70	141.30	-11.10	212.22	VA 50L	VANIMO	NGDC & IPS
-19.30	146.70	-28.55	219.88	TV 51R	TOWNSVILLE	NGDC & IPS
35.70	139.50	28.22	210.12	TO 535	KOKUBUNJI	NGDC
39.70	140.10	32.30	210.77	AK 539	AKITA	NGDC
-35.30	149.00	-45.75	225.63	CB 53N	CANBERRA	NGDC & IPS
45.40	141.70	38.14	212.11	WK 545	WAKKANAI	NGDC
-42.90	147.20	-54.22	225.66	HO 54K	HOBART	NGDC & IPS
-29.00	168.00	-35.82	245.27	NI 63!	NORFOLK IS	NGDC & IPS
-17.70	210.70	-16.20	284.63	TT 71P	TAHITI	NGDC
20.80	203.50	21.55	270.27	MA 720	MAUI	NGDC
35.60	239.40	41.49	301.80	PA 836	POINT ARGUELLO	NGDC
40.00	254.70	49.14	317.93	BC 840	BOULDER	NGDC
45.10	283.80	56.95	358.08	OT 945	OTTAWA	NGDC
58.80	265.80	69.70	329.29	CH 958	CHURCHILL	NGDC
74.70	265.10	83.92	312.49	RB 974	RESOLUTE BAY	NGDC
14.80	342.60	4.66	58.26	DK A14	DAKAR	NGDC

NGDC and because we encountered no instances where ionosonde data was clearly erroneous or inconsistent.

Station	f_oF_2						f_oE					
	2	3	4	5	6	9	2	3	4	5	6	9
OU 012	★	★	★	☆	☆	☆	☆	☆	☆	☆	☆	☆
LE 038	★	★	●	●	●	●	☆	☆	☆	☆	☆	☆
RO 041	●	●	●	●	●	●	★	☆	☆	☆	★	☆
PT 046	●	●	●	●	●	●	★	☆	☆	☆	★	☆
LN 047	●	●	★	●	★	★	☆	☆	☆	★	★	★
SL 051	●	●	●	●	●	●	☆	★	★	★	★	★
PE 054	●	●	●	●	●	●						
JR 055	●	●	●	●	●	●	●	●	●	●	●	●
JO 120	☆	☆	★	★	★	☆						
UP 158	★	●	●	★	★	●	☆	★	☆	☆	☆	☆
LY 164	★	★	★	●	★	★	☆	☆	☆	☆	☆	☆
SO 166	★	★	★	★	★	★						
KI 167	☆	☆	☆	☆	☆	☆						
LR 22J	●	●	●	●	●	●	★	★	★	★	★	★
DW 41K												
OK 426												
YG 431												
MU 43K	●	●	●	●	●	●	★	★	★	★	★	★
VA 50L	★	★	★	★	★	★	☆	☆	☆	★	☆	★
TV 51R	★	●	●	★	●	★	★	☆	☆	☆	☆	☆
TO 535	●	●	●	★	●	●	☆	☆	☆	☆	☆	☆
AK 539												
CB 53N	●	●	●	●	●	●	★	★	★	★	★	★
WK 545												
HO 54K	●	●	●	●	●	●	☆	★	☆	☆	☆	☆
NI 63!	★	☆	●	●	●	☆	☆	☆	★	★	★	☆
TT 71P	★	★	★	★	★	●	☆	★	☆	★	☆	★
MA 720	●	●	★	●	●	●	☆	☆	☆	☆	☆	☆
PA 836	●	●	●	●	●	●	☆	☆	☆	★	☆	☆
BC 840	●	●	●	●	●	●	☆	☆	☆	☆	☆	☆
OT 945	★	☆	☆			☆	★	☆	☆	☆	☆	☆
CH 958	★	☆	★	★	★		☆	☆	☆	☆	☆	☆
RB 974	★	☆	☆	★	★	☆		☆	☆	☆	☆	☆
DK A14	★	★	★	☆	★	★	☆	☆	☆	☆	☆	☆

Figure 2. Analog ionosonde f_oF_2 and f_oE data availability for 2-6 and 9 October. The symbol ● indicates 24 hourly values, ★ indicates 12-23 values, and ☆ indicates 1-11 values.

2.2 Digisondes

The Digisonde is an automated digital ionosonde developed at the University of Massachusetts, Lowell (formerly Lowell University) by Prof. Bodo Rheinisch and colleagues. They also developed the ARTIST software which automatically scales the digital ionograms and performs a true height analysis [*Reinisch and Huang,* 1983]. We believe the Digisonde data to be of generally high quality, although the nighttime E-layer data may be problematic. The values of both f_oE and h_mE often appear to be artifical (e.g., $f_oE = 0.61$ and $h_mE = 110$ km), presumably because the software was unable to determine the actual values. For PRISM validation we ignored the E region data whenever h_mE had the value 110.000 km. Otherwise, all available Digisonde data was used without qualification.

The locations of the five Digisondes whose data were supplied to us are listed in Table 3. They form a rough chain along the coast of North America. Note that the two and three character station codes for the Digisondes were assigned by us for ease and uniformity of identification of data and model output. Although chosen by the same criteria used by the World Data Center for selecting analog ionosonde identifiers, they are in no way "official."

Table 3. The five Digisonde sites used for PRISM validation. The "Station codes" were assigned by us (not by WDC) and are in no way "official."

Geographic		Geomagnetic		Station	
lat	lon	lat	lon	codes	Station Name
42.60	288.50	54.19	4.69	MH J43	Millstone Hill
37.90	284.50	49.83	358.27	WP 937	Wallops Island
53.30	299.70	62.88	22.86	GS J53	Goose Bay
32.20	295.60	42.93	12.90	BX J32	Bermuda
47.30	306.00	55.52	29.18	AG J47	Argentia

Unfortunately, most of the Digisondes were not operating during the period 2-6 October. Millstone Hill operated throughout 2 October and until 0200 UT on 3 October, providing hourly data. From 1830 UT on 5 October until 0000 UT on 6 October, it returned 15 minute data. It provided hourly data throughout 6 October. The other four Digisondes did not operate at all during 2-4 October, and only at irregular or sporadic intervals on 5 and 6 October. Since the analog ionosonde data did not include any true height analysis, we were most anxious to run PRISM with as much Digisonde height data as possible, even in the absence of ISR data.

Therefore, we chose to use data from 9 October when all five Digisondes were operating on a regular schedule throughout the day.

2.3 Polarimeters

We received data from four polarimeters operated by Phillips Laboratory (PL/GPIM) along the east coast of North America. The polarimeters measure the Faraday rotation produced by the combination of ionospheric plasma and magnetic field along the line of sight from the polarimeter to the GOES satellite whose transmissions they monitor. The Faraday rotation can be converted into total electron content (TEC) along the line of site. This slant TEC is a measure of the electron content up to about 2000 km altitude. We converted the slant TEC to an equivalent TEC by multiplying the slant TEC by the sine of the elevation angle of the line of sight. The vertical TEC values are assumed to represent the TEC at the "ionospheric intersection point," generally defined as the location of the centroid of the electron density profile along the line of sight. In midlatitudes, a good approximation to this altitude is 420 km, and this is what we used to define the locations of the ionospheric intersection of each polarimeter. The coordinates of the ionospheric interesection of each polarimeter are listed in Table 4.

Table 4. The ionospheric intersection coordinates of the four polarimeter used for PRISM validation.

Geographic		Geomagnetic		Station	
lat	lon	lat	lon	codes	Station Name
45.00	276.00	56.90	346.46	GP 944	Goose Bay
38.00	277.00	49.99	347.60	HM 939	Hamilton
17.00	284.00	29.28	355.39	RP 917	Ramey
26.00	280.00	38.20	350.90	KK 925	Kennedy

The polarimeter TEC data has been carefully checked for quality by Pat Doherty of Boston College, so we consider this very reliable data. The data is in the form of 15 minute TEC values, from which we selected hourly values to conform to the hourly analog ionosonde data. PRISM uses the TEC data along with its own profile shape to derive an estimate of N_mF_2 and f_oF_2.

2.4 ISR Data

We received data from four ISR sites, however, one of the sites was operating in a mode that rendered the data unsuitable for PRISM validation. The three sites whose data we used are listed in Table 5 along with the start and stop times of the data. The data was supplied in the form of vertical profiles with electron density given at 40 km intervals from 0 to 580 km altitude. The profiles are supplied at hourly intervals on each half hour (i.e., 0030, 0130, 0230, ...) throughout the period of operation. The radars were scanning in elevation and azimuth, and the data was selected so that the elevation angle was greater than 70^{o}. The data was binned and averaged in both time and space, so the profiles are not instantaneous snapshots of the ionosphere. Furthermore, the relatively low altitude resolution precludes use of the data for E-layer validation.

Table 5. The three ISR sites used for PRISM validation.

Geographic lat	Geographic lon	Geomagnetic lat	Geomagnetic lon	Station codes	Station Name	Start time on 2 Oct	Stop time on 6 Oct
18.30	293.25	30.16	7.47	AR J19	Arecibo	1300 UT	2000 UT
42.60	288.50	54.19	4.69	MH J43	Millstone Hill	2000 UT	2000 UT
67.00	309.00	74.09	42.74	SM J67	Sondrestrom	1000 UT	1800 UT

For the actual validation runs whose statistics are reported here, none of the ISR data was used to drive PRISM or ICED, but was used solely as "ground truth," i.e., to compare with model calculations. However, we did use this data to simulate a complete set of F-layer data (f_oF_2, h_mF_2, and in situ density and temperature at 580 km) in order to illustrate the operation of the PRISM adjustment algorithm. This is described in the next section (**3. Data Usage**).

2.5 SSIES in situ Plasma Data

DMSP satellites F8 and F9 were both operating during October 1989. Unfortunately, neither the Langmuir probe (electron density and temperature) nor the Retarding Potential Analyzer (ion composition, ion temperature, ion drift velocity) were operating, so the only data available are from the Scintillitation Meter (total ion density and fluctuations) and the Drift Meter (ion drift velocity). PRISM is designed to use the ion drift velocity to locate the equatorward edge of the midlatitude or subauroral trough, and to use the in situ electron density and electron

and ion temperatures to adjust it topside profiles. (The temperatures are used to derive a scale height, assuming diffusive equilibrium.) Nevertheless, in the absence of temperature, PRISM can still use the electron density (= total ion density) to adjust its topside profiles. Unfortunately, since the ISR data stops at 580 km, and DMSP operates at 840 km, there is no real "ground truth" for the topside adjustment. Consequently, this data was used primarily to verify that PRISM ingests and uses the data properly.

We were given access to the processed data tapes along with software for reading the tapes and extracting the desired data. We modified that software to extract only the data we needed (ion drift and total ion density) and write text files containing the ephemeris information along with the desired data. We then wrote software to extract data for a particular time period (generally the 110 minute period just prior to the UT for which an ionospheric specification is desired). The ephemeris information was given at one minute intervals while the data itself was given at one second intervals. Consequently, we interpolated the ephemeris information assuming that the satellite was in a circular orbit so that the satellite motion along the orbit was uniform. The ion drift data used as 5 second averages, which gives a spatial resolution of about 37 km (at the satellite altitude of 840 km). The total ion density was used as 30 second averages, which gives a spatial resolution of about 223 km.

In order to assess the impact of SSIES data on PRISM performance, we searched for close overflights of the ISR sites by either of the DMSP satellites. During the 2-6 October period, there were disappointingly few close overflights. The best such overflight occurred at 1355:41 UT when F9 crossed the latitude of Arecibo (18°18') about 1.8° (or 190 km) west of Arecibo. This event is reported below.

2.6 SSJ/4 Particle Precipitation Data

The DMSP F8 and F9 satellites also carried SSJ/4 sensors to measure precipitating electrons and ions with energies in the range 30 eV to 30 keV. We were given access to the data tapes containing ephemeris information and raw counts in each electron and ion channel. Based on information in *Hardy et al.* [1984] and additional information provided by F. Rich of PL/GPSG, we converted the counts to electron flux, then summed over channels to get a total number flux, J, and summed over the energy weighted channels to get a total energy flux, Q. The ratio J/Q gives the mean energy, $\overline{E}$. PRISM uses Q to locate the precipitation boundaries,

and both Q and $\overline{E}$ to determine the auroral E layer parameters. We found that the SSJ/4 data was rather noisy at low values of the number flux (due to the small number of counts recorded per accumulation time). We handled this by rejecting data for which the statistical uncertainty was greater than one-half the value itself. This allowed us to retain the full spatial resolution of 7 km (at an altitude of 110 km). However, an alternative approach would have been to take 5 second averages. This still allows a spatial resolution of 33 km.

Since there was very little high latitude data available for use as "ground truth," the SSJ/4 data were used primarily to demonstrate that PRISM could ingest and use such data.

3. Data Usage

We spent a considerable amount of time selecting which data were to be used to drive PRISM and ICED and which data were to be held back as "ground truth." The ionosonde driver stations (analog and digital) were selected to provide a reasonably uniform global coverage within the constraints imposed by the highly non-uniform distribution of the overall set of stations. Since there are to be 19 DISS (Digital Ionospheric Sounding System) sites, we selected 19 ionosondes from the combined list of analog and digital sounders. For the 2-6 October period, we selected the only available digital sounder (Millstone Hill) and 18 analog sounders. The analog ionosondes were chosen from the set of stations that reported f_oF_2 values more than half the time. With all five Digisondes available on 9 October, we selected four as drivers and added 15 of the analog ionosondes to form the required 19 driver sites. For both periods we selected three of the four polarimeters as drivers and used the other one as ground truth. The two sets of driver sites (one for 2-6 October and the other for 9 October) are listed in Table 6. The two sets of ground truth stations are listed in Table 7.

Table 6. The driver sites for 2-6 and 9 October 1989. ("II" indicates "ionospheric intersection" for polarimeters.)

2-6 October		9 October	
codes	Station Name	codes	Station Name
OU 012	OUAGADOUGOU	LE 038	LISBONNE
LE 038	LISBONNE	RO 041	ROME
RO 041	ROME	SL 051	SLOUGH
PT 046	POITIERS	PE 054	ST PETER-ORDING
SL 051	SLOUGH	UP 158	UPPSALA
PE 054	ST PETER-ORDING	SO 166	SODANKYLA
LY 164	LYCKSELE	LR 22J	LA REUNION
LR 22J	LA REUNION	VA 50L	VANIMO
MU 43K	MUNDARING	TO 535	KOKUBUNJI
VA 50L	VANIMO	CB 53N	CANBERRA
TO 535	KOKUBUNJI	TT 71P	TAHITI
HO 54K	HOBART	MA 720	MAUI
NI 63!	NORFOLK IS	PA 836	POINT ARGUELLO
TT 71P	TAHITI	RB 974	RESOLUTE BAY
MA 720	MAUI	DK A14	DAKAR
PA 836	POINT ARGUELLO	GS J53	Goose Bay
CH 958	CHURCHILL	MH J43	Millstone Hill
RB 974	RESOLUTE BAY	BX J32	Bermuda
MH J43	Millstone Hill	AG J47	Argentia
GP 944	Goose Bay (II)	GP 944	Goose Bay (II)
HM 939	Hamilton (II)	HM 939	Hamilton (II)
RP 917	Ramey (II)	RP 917	Ramey (II)

Table 7. The "ground truth" sites for 2-6 and 9 October 1989.

2-6 October		9 October	
codes	Station Name	codes	Station Name
LN 047	LANNION	OU 012	OUAGADOUGOU
JR 055	JULIUSRUH/RUGEN	PT 046	POITIERS
UP 158	UPPSALA	LN 047	LANNION
KI 167	KIRUNA	JR 055	JULIUSRUH/RUGEN
TV 51R	TOWNSVILLE	LY 164	LYCKSELE
CB 53N	CANBERRA	KI 167	KIRUNA
BC 840	BOULDER	MU 43K	MUNDARING
OT 945	OTTAWA	TV 51R	TOWNSVILLE
DK A14	DAKAR	HO 54K	HOBART
KK 925	Kennedy (II)	NI 63!	NORFOLK IS
		BC 840	BOULDER
		OT 945	OTTAWA
		WP 937	Wallops Island
		KK 925	Kennedy (II)

In addition to the real-time ionospheric data described above, PRISM requires an estimate of solar activity, either $F_{10.7}$ or sunspot number (*SSN*), and K_p, an indicator of geomagnetic activity. The values we used for 2-6 and 9 October have already been displayed in Table 1. ICED makes no direct use of real-time data, but does require an effective sunspot number (SSN_{eff}) and Q, a magnetic activity index related to the equatorward edge of the auroral oval at local midnight. If real-time ionosonde data is available, PRISM calculates its own estimate of SSN_{eff} internally.

At AFSFC, SSN_{eff} will be calculated every hour or one-half hour from DISS f_oF_2 data. The algorithm for that calculation is under development at NGDC. For this study, we used a copy of the FORTRAN program SSNE (which was developed at NGDC) supplied by ETAC. SSNE accepts ionosonde f_oF_2 data in NGDC standard format and calculates the effective sunspot number subject to various user selectable conditions. The data may be weighted by region (high, middle, or low latitude) and by local time (day or night). Each station may be weighted individually. In addition, the data used can be restricted to a rectangular region of latitude and longitude. For these runs, we chose a global region and weighted the data as follows:

region: 1.0 for midlatitudes, 0.5 for high and low latitudes
local time: 1.0 for day, 0.5 for night

Otherwise, all stations were weighted equally. The resulting effective sunspot numbers for 2-6 and 9 October 1989 are displayed in Table 8.

Table 8. Effective Sunspot Numbers (SSN_{eff}) for 2-6 and 9 October 1993.

UT	2	3	4	5	6	9
00:00	157.3	148.3	157.1	160.4	163.8	178.9
01:00	150.7	148.1	158.9	162.4	164.2	185.2
02:00	148.0	149.9	162.4	165.7	166.7	190.1
03:00	145.9	150.7	164.4	167.5	167.6	192.8
04:00	145.9	150.8	164.7	169.9	169.8	192.9
05:00	145.5	150.3	165.3	170.8	169.9	190.0
06:00	142.9	150.2	164.7	171.7	170.0	186.0
07:00	142.6	151.1	163.6	171.3	171.3	181.7
08:00	142.5	151.4	162.7	170.5	169.7	179.2
09:00	143.0	152.7	162.8	170.6	170.3	175.4
10:00	141.7	151.5	160.4	168.7	168.6	171.5
11:00	141.8	152.0	159.3	169.0	168.0	170.5
12:00	142.9	152.8	159.9	169.4	168.7	171.0
13:00	141.4	151.0	157.9	168.4	168.3	169.0
14:00	139.0	147.6	153.5	164.2	166.8	166.3
15:00	137.7	145.2	150.8	161.5	164.9	165.0
16:00	136.6	143.3	148.9	158.0	161.9	165.8
17:00	137.6	144.2	149.4	156.6	161.2	165.9
18:00	138.4	145.5	150.2	155.5	160.7	165.2
19:00	140.9	148.3	151.6	155.2	160.1	165.8
20:00	143.5	150.0	155.1	157.0	161.5	167.3
21:00	144.8	152.0	157.6	158.1	162.6	171.2
22:00	148.9	156.9	161.0	161.7	165.4	174.7
23:00	149.1	157.4	160.9	163.5	166.6	178.5

At AFSFC, the auroral Q index is currently calculated from K_p according to a formula provided by Kevin Scro of AFSFC:

$$Q = 1.51K_p - 1.74 \tag{1}$$

At AFSFC "pseudo K_p" values will be calculated at least hourly based on real-time magnetometer data. For this validation study, however, we used the "official" 3-hour K_p values as published by NGDC. The Q values for 2-6 and 9 October 1989 are displayed in Table 9. The SSN_{eff} and Q values listed in Tables 8 and 9 were the sole input used for all the ICED runs presented here. For

PRISM runs, the inputs were $F_{10.7}$ and K_p, listed in Table 1, the same SSN_{eff} values used for ICED, and the various "real-time" ionospheric measurements described in the **Data Acquisition** section. When no "real-time" data was input to PRISM, it used SSN_{eff}. When "real-time" ionosonde data was input, PRISM calculated its own SSN_{eff} internally and ignored the input value.

Table 9. Effective Auroral Q Index for 2-6 and 9 October 1989.

UT	2	3	4	5	6	9
00-02	0.27	-0.73	1.28	1.78	1.28	3.29
03-05	3.80	-0.23	1.28	-0.23	-0.23	3.80
06-08	2.29	1.28	-0.23	-1.74	1.28	1.78
09-11	1.28	2.29	-0.73	-0.23	2.29	0.78
12-14	1.28	3.80	1.28	1.28	2.29	1.28
15-17	1.78	3.29	1.78	-0.23	2.79	0.27
18-20	0.78	3.80	-0.23	-0.23	1.78	1.28
21-23	-0.23	1.78	1.28	0.78	2.79	2.79

4. PRISM F Region Adjustments

Since we did not have good topside "ground truth" (the DMSP data being at 840 km while the ISR data being confined below 580 km), we first demonstrated PRISM's ability to use topside date using simulated ionosonde and in situ data based on the ISR data. That is to say, from an ISR EDP, we derived f_oF_2, h_mF_2, and the density and temperature at 580 km. (Due to the rather low altitude resolution of the ISR data, we did not attempt to derive any E region parameters.)

While it is straightforward to derive the first three parameters from an EDP, the temperature is more difficult. PRISM ingests the electron and ion temperatures (T_e and T_i, respectively) separately, so we derived simulated temperatures using

$$T_p = \frac{mgH}{k} \tag{2}$$

where m is the ion mass, g is the local acceleration due to gravity, H is the scale height derived from the ISR data, k is Boltzmann's constant, and $T_p = T_e + T_i$ is the plasma temperature. We further assumed $T_e = 2T_i$, so $T_i = \frac{1}{3}T_p$. Since PRISM calculates the scale height from

$$H = \frac{kT_p}{mg} \tag{3}$$

it derives the same scale height we started with. (Of course, this procedure does not test the validity of our working assumption that the topside ionosphere is in diffusive equilibrium.)

The results are shown in Figure 3 for 1800 UT on 4 October 1989 at Arecibo. (The local time was about 1330.) Four cases are displayed in the Figure, and the associated statistics are displayed in Table 10. In all four cases the effective sunspot number (SSN_{eff}) and auroral Q index (described in the previous section) were used as input to ICED. In case (a), the only inputs to PRISM were the same effective sunspot number, the daily $F_{10.7}$ value, and the appropriate K_p value. In case (b) that input data was augmented by the f_oF_2 value derived from the peak density in the ISR profile. h_mF_2 was added to PRISM input for case (c), and in case (d), the topside data (density and scale height at 580 km) were added.

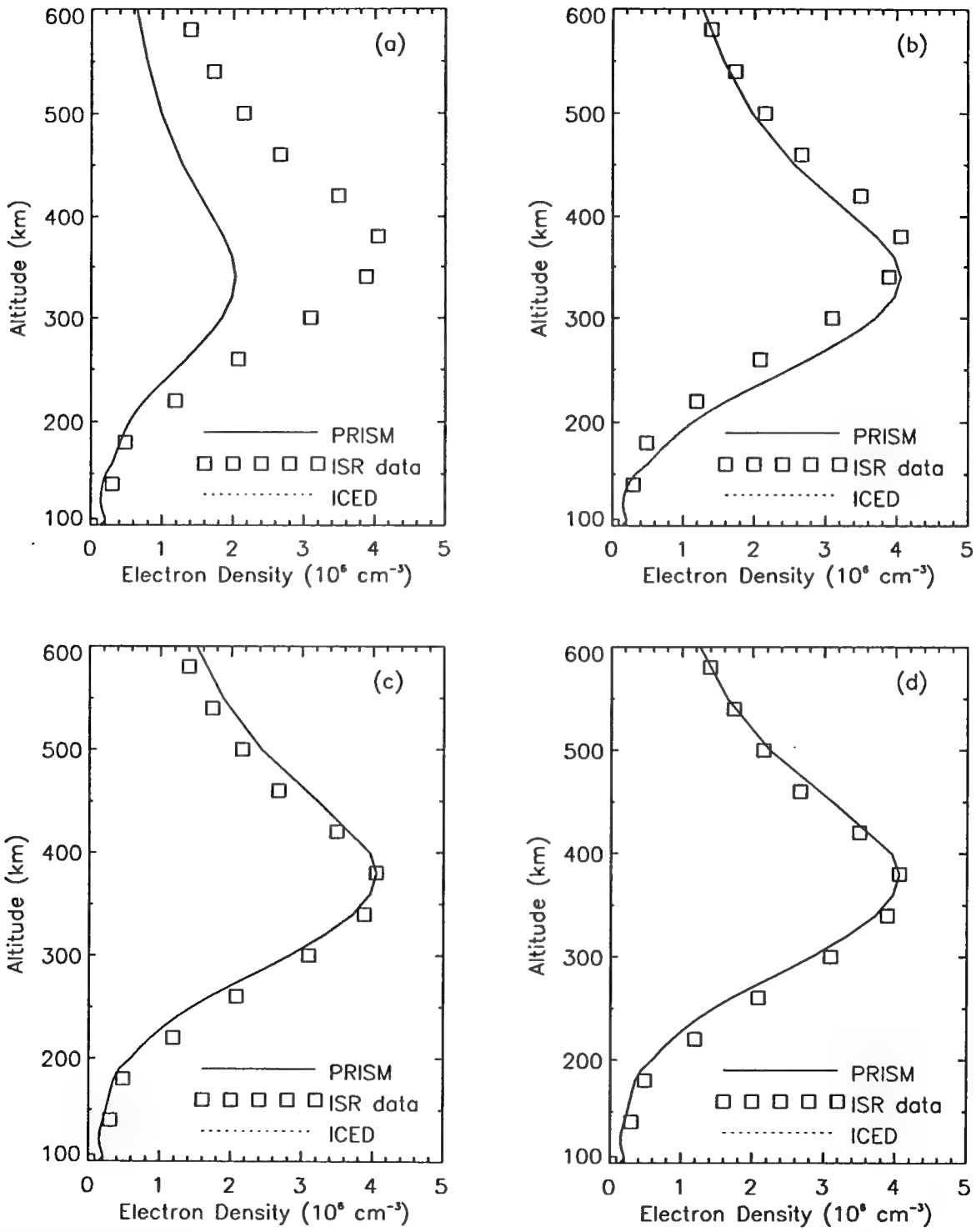

Figure 3. PRISM performance using input data simulated from ISR data. (a) no data, (b) peak density only, (c) peak density and altitude, (d) peak and topside data.

Not surprisingly, in case (a) PRISM and ICED performed about equally well. Note that the peak density predicted by climatology is 2×10^6 cm^{-3}, while the actual peak density is twice that value. In order to quantify model performance, we introduce two measures of model error relative to the data. The first, RMS density error, is the root mean square error in model density relative to the data at the 13 ISR data altitudes between 100 and 600 km. Specifically,

$$\text{RMS density error} = \sqrt{\frac{1}{13}\sum_{k=1}^{13}\left[\frac{N_m(z_k)-N_d(z_k)}{N_d(z_k)}\right]^2} \tag{4}$$

where $N_m(z_k)$ is the model electron density at altitude z_k and $N_d(z_k)$ is the data value at that same altitude.

The second performance measure is the error in "TEC." Since there is ISR data only below 600 km, the "TEC" obtained from the data is really the electron content between 100 and 600 km. Perhaps a better term would be "PEC" (Partial Electron Content)! First we define TEC_s

$$\text{TEC}_s = \int_{100\text{ km}}^{600\text{ km}} N_s(z)\,dz \tag{5}$$

where s can be m for "model" or d for "data". Then the "TEC" error is

$$\text{TEC error} = \frac{\text{TEC}_m - \text{TEC}_d}{\text{TEC}_d} \tag{6}$$

In order to quantify the comparison with ICED, we have also defined the PRISM "Improvement" as

$$\text{PRISM Improvement} = \frac{\text{ICED error} - \text{PRISM error}}{\text{ICED error}} \tag{7}$$

Note that the most improvement that can be obtained is 100% (when the PRISM error vanishes).

These performance measures are summarized in Table 10 for the four cases displayed in Figure 3. From the figure and the table, it is clear that most of the PRISM improvement comes

from specifying the peak density, as in case (b). Adding the height of the peak produces further improvement, especially in the RMS density error. Adding the topside data produces only a small reduction in error. However, it is important to note that SSIES data is taken at 840 km rather than 580 km, and since the ISR data stopped below 600 km, we cannot assess the impact on true TEC. This test was primarily intended as a demonstration of PRISM's ability to utilize both ground based and satellite based data, not as an assessment of the relative value of the two.

Table 10. PRISM performance using peak and topside data simulated from ISR data. (Arecibo, 1800 UT, 4 Oct 1989)

	PRISM error		ICED error		"Improvement"	
Data Used	density	"TEC"	density	"TEC"	density	"TEC"
(a) none	46%	-48%	44%	-44%	-1%	-1%
(b) f_oF_2	25%	4%	44%	-44%	43%	92%
(c) f_oF_2 & h_mF_2	18%	1%	44%	-44%	59%	99%
(d) f_oF_2, h_mF_2, & topside	16%	-3%	44%	-44%	64%	94%

5. F Region Validation

As described above, whenever possible, the available data was divided into "driver" and "ground truth" data sets. The "driver" data was used to drive the models, either directly as input to PRISM, or indirectly as in the calculation of SSN_{eff} for ICED. The "ground truth" data was not used as input into either of the models, but was used exclusively as an independent check on model performance. However, we point out that because ICED is not driven directly by ionosonde data, but uses a single least square parameter, SSN_{eff}, it cannot reproduce the "driver" ionosonde data (except in the case where there is only one ionosonde station). PRISM, on the other hand is designed to reproduce the input data nearly exactly (in low and middle latitudes). Consequently, comparisons between PRISM and ICED values and the driver data are meaningful because they demonstrate that difference between the models. This can be important when AFSFC is supporting a customer who happens to be colocated with a DISS or a TISS site. ICED will almost invariably return a value for f_oF_2 or TEC at the customer's site that differs from the local DISS or TISS value. PRISM, on the other hand, will almost always return the observed value, which will reassure the customer that the ionospheric information he is receiving from AFSFC is relevant to his needs. Therefore, in this and the following sections, we display comparisons between the two models and "driver" data, "ground truth" data, and the combined data set.

5.1 f_oF_2 Validation

Because much of the historical data consists of critical frequencies (mostly f_oF_2) hand scaled from analog ionograms, much of our validation effort has gone into f_oF_2 validation. Fortunately, as we demonstrated in the previous section, f_oF_2 is not only a critical frequency, but a critical parameter in real-time ionospheric specification since its specification provides the greatest reduction in EDP error.

All of the f_oF_2 validation runs were done the same way. For each UT on each day of the period 2-6 October and 9 October, f_oF_2 data from the driver stations was used to calculate SSN_{eff} for ICED and was placed in an input file for use by PRISM. The auroral Q index was calculated from K_p for use by ICED, while K_p itself was used by PRISM. TEC from the three driver polarimeter sites was also placed in an input file for PRISM's use. (We ran all the cases with and without TEC data and found no significant difference in PRISM performance, primarily due to the

small number of polarimeters, so all the results presented here include TEC as input. Since PRISM converts TEC into f_oF_2, this is the appropriate place for TEC data use.)

For each UT during the stated period, we calculated the difference between the model values of f_oF_2 and N_mF_2 and the ionosonde data. The f_oF_2 errors are always expressed in MHz, and the N_mF_2 errors are always expressed as a percentage of the data value. To characterize PRISM and ICED performance for a given UT, the RMS errors for (1) "driver" stations, (2) "ground truth" stations, and (3) all stations were calculated. To characterize model performance for a given day, the same procedure is followed: RMS errors were calculated across each class of station and over all 24 UT's. Finally, to characterize model performance for the entire validation period, RMS errors were calculated across all stations, and all UT's during the six day period. We will first look at overall model performance, then the day to day performance, and finally, examine some specific UT's.

The overall comparison between PRISM and ICED for the six validation days is presented in Table 11. The "Improvement" measure is defined in the previous section, and is simply the ICED error less the PRISM error expressed as a percentage of the ICED error. The Midlatitude Statistics are based on those stations which fall within PRISM's low and midlatitude region. The Global Statistics are based on all stations regardless of latitude. (Because PRISM uses a least squares fitting method for the high latitude adjustment, it does not produce zero error at high latitude sites, which results in global "driver" RMS errors that are different from zero.)

It is clear that while PRISM does significantly better than ICED at reproducing the driver data, its performance is comparable to ICED's where there is little or no driver data. This is not surprising since the ionospheric correlation length is of the order of a thousand kilometers, and any improvement due to real-time data will fade away as one moves away from a driver site.

Table 11. Summary of PRISM and ICED validation results for 2-6 and 9 October 1989.

Quantity	Station Hours	RMS Errors		PRISM Improvement
		ICED	PRISM	
Midlatitude Statistics:				
all stations:				
RMS f_oF_2 error (Mhz):	2840	1.5	0.5	63%
RMS N_mF_2 error (%):	2840	36%	17%	53%
driver stations:				
RMS f_oF_2 error (MHz):	1959	1.6	0.0	97%
RMS N_mF_2 error (%):	1959	39%	1%	97%
ground truth stations:				
RMS f_oF_2 error (MHz):	881	1.1	1.0	10%
RMS N_mF_2 error (%):	881	29%	30%	-6%
Global Statistics:				
all stations:				
RMS f_oF_2 error (MHz):	3137	1.5	0.7	54%
RMS N_mF_2 error (%):	3137	40%	20%	50%
driver stations:				
RMS f_oF_2 error (MHz):	2159	1.6	0.4	73%
RMS N_mF_2 error (%):	2159	44%	13%	70%
ground truth stations:				
RMS f_oF_2 error (MHz):	978	1.1	1.0	5%
RMS N_mF_2 error (%):	978	30%	31%	-5%

The daily comparisons of PRISM and ICED performance in terms of global and midlatitude f_oF_2 and N_mF_2 errors are displayed in Tables 12, 13, 14, and 15. We see the same pattern as in the overall summary: PRISM does a much better job of reproducing the input data, but away from the driver sites, PRISM's performance is comparable to ICED's. Some days are better than others, but overall, PRISM provides a substantial improvement in ionospheric specification.

Table 12. Daily *Global* Statistics of f_oF_2 Errors.

Date	Station Type	Station Hours	RMS Errors		PRISM "Improvement"
			ICED	PRISM	
2 Oct	driver	375	1.4	0.2	86%
	other	175	0.9	0.9	3%
	all	550	1.3	0.5	59%
3 Oct	driver	323	1.7	0.4	76%
	other	162	1.0	1.1	-8%
	all	485	1.5	0.7	55%
4 Oct	driver	342	1.8	0.2	89%
	other	150	1.2	1.0	17%
	all	492	1.6	0.5	67%
5 Oct	driver	367	1.6	0.2	88%
	other	146	1.1	0.9	19%
	all	513	1.5	0.5	66%
6 Oct	driver	356	1.7	0.6	65%
	other	151	1.2	1.2	1%
	all	507	1.6	0.8	50%
9 Oct	driver	396	1.6	0.7	56%
	other	194	1.2	1.2	0%
	all	590	1.5	0.9	40%

Table 13. Daily *Midlatitude* Statistics of f_oF_2 Errors.

Date	Station Type	Station Hours	RMS Errors		PRISM "Improvement"
			ICED	PRISM	
2 Oct	driver	340	1.4	0.0	98%
	other	159	0.9	0.9	4%
	all	499	1.3	0.5	62%
3 Oct	driver	295	1.7	0.0	98%
	other	146	1.0	1.0	5%
	all	441	1.5	0.6	59%
4 Oct	driver	317	1.8	0.0	99%
	other	134	1.2	1.0	19%
	all	451	1.6	0.5	68%
5 Oct	driver	337	1.6	0.0	99%
	other	130	1.1	0.9	20%
	all	467	1.5	0.5	69%
6 Oct	driver	320	1.7	0.0	98%
	other	132	1.2	1.0	15%
	all	452	1.6	0.5	65%
9 Oct	driver	350	1.6	0.1	93%
	other	180	1.2	1.2	1%
	all	530	1.5	0.7	54%

Table 14. Daily *Global* Statistics of N_mF_2 Errors.

Date	Station Type	Station Hours	RMS Errors		PRISM "Improvement"
			ICED	PRISM	
2 Oct	driver	375	47%	7%	85%
	other	175	31%	31%	0%
	all	550	42%	18%	57%
3 Oct	driver	323	52%	14%	73%
	other	162	26%	26%	0%
	all	485	45%	19%	58%
4 Oct	driver	342	49%	4%	91%
	other	150	28%	27%	2%
	all	492	44%	15%	66%
5 Oct	driver	367	36%	6%	82%
	other	146	29%	30%	-1%
	all	513	35%	16%	53%
6 Oct	driver	356	41%	17%	59%
	other	151	30%	30%	-1%
	all	507	38%	21%	44%
9 Oct	driver	396	38%	20%	46%
	other	194	32%	38%	-18%
	all	590	36%	27%	24%

Table 15. Daily *Midlatitude* Statistics of N_mF_2 Errors.

Date	Station Type	Station Hours	RMS Errors		PRISM "Improvement"
			ICED	PRISM	
2 Oct	driver	340	33%	1%	98%
	other	159	26%	29%	-14%
	all	499	31%	16%	47%
3 Oct	driver	295	42%	1%	98%
	other	146	27%	25%	6%
	all	441	37%	15%	61%
4 Oct	driver	317	48%	0%	99%
	other	134	28%	26%	5%
	all	451	43%	14%	66%
5 Oct	driver	337	37%	0%	99%
	other	130	30%	30%	-1%
	all	467	35%	16%	55%
6 Oct	driver	320	35%	1%	98%
	other	132	30%	29%	1%
	all	452	33%	16%	52%
9 Oct	driver	350	37%	3%	92%
	other	180	31%	38%	-22%
	all	530	35%	22%	37%

Let us now examine one day in somewhat greater detail. The midlatitude driver RMS errors in f_oF_2 and N_mF_2 are displayed in Figure 4. As expected, PRISM's RMS error is very small indicating that it is reproducing the driver data. In contrast, ICED's RMS N_mF_2 error varies from a low of 20% to a high of 100%, while the RMS f_oF_2 error varies from 1 to 3 MHz. The statistics for the "ground truth" stations are displayed in Figure 5. As expected, PRISM and ICED have about the same RMS errors, ranging from 10% to 60% in N_mF_2 and 0.4 MHz to 1.7 MHz in f_oF_2. Finally, in Figure 6 we show the statistics using *all* the stations, which gives a qualitative indication of PRISM's overall performance.

It is not clear why ICED does better against the "ground truth" stations than against the driver stations. However, ICED's f_oF_2 values come from the URSI coefficient set, which was derived from data from a specific set of ionosonde stations. It may be that the "ground truth" stations are more representative of the URSI stations than the "driver" stations are. Hence, the effective sunspot number derived from the "driver" data may not be the best value from ICED's point of view. While PRISM does normalize its f_oF_2 values to the URSI coefficients before performing its real-time adjustments, the real-time adjustment process guarantees that PRISM will reproduce the driver data (from low and mid-latitudes).

Now let us examine PRISM and ICED performance at 0700 UT, when PRISM performed worst against "ground truth" data, and at 1300 UT, when PRISM performed best. It is interesting to note that at 0700 UT ICED performed at its best on the driver data but at its worst on the "ground truth" data. The opposite was true at 1300 UT. A contour plot of PRISM's N_mF_2 errors at 0700 UT is shown in Figure 7, while the corresponding plot for ICED is in Figure 8. (Since the contours are based on a very sparse and irregularly distributed data set, their precise shape should not be taken too seriously.) For this UT, PRISM and ICED produce roughly comparable results, although ICED is decidedly worse over Europe (approx. 60°E magnetic longitude).

Figures 9 and 10 show the same plots but for 1300 UT. For this UT the differences between the two models is much more pronounced, with PRISM showing a much lower error overall.

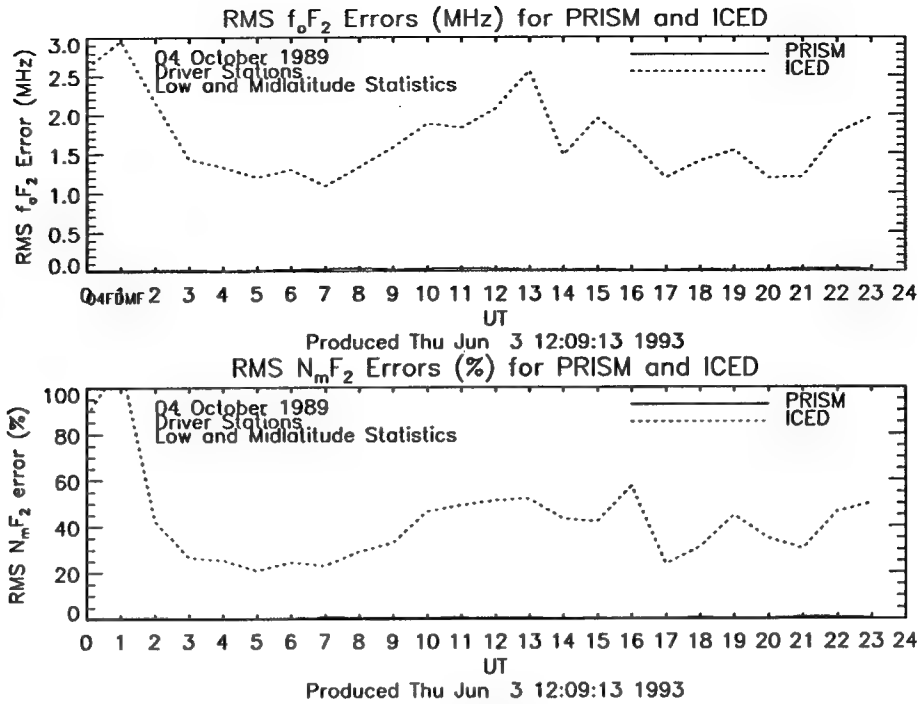

Figure 4. Hourly Midlatitude *"Driver"* Statistics for f_oF_2 and N_mF_2 errors for 4 October 1989.

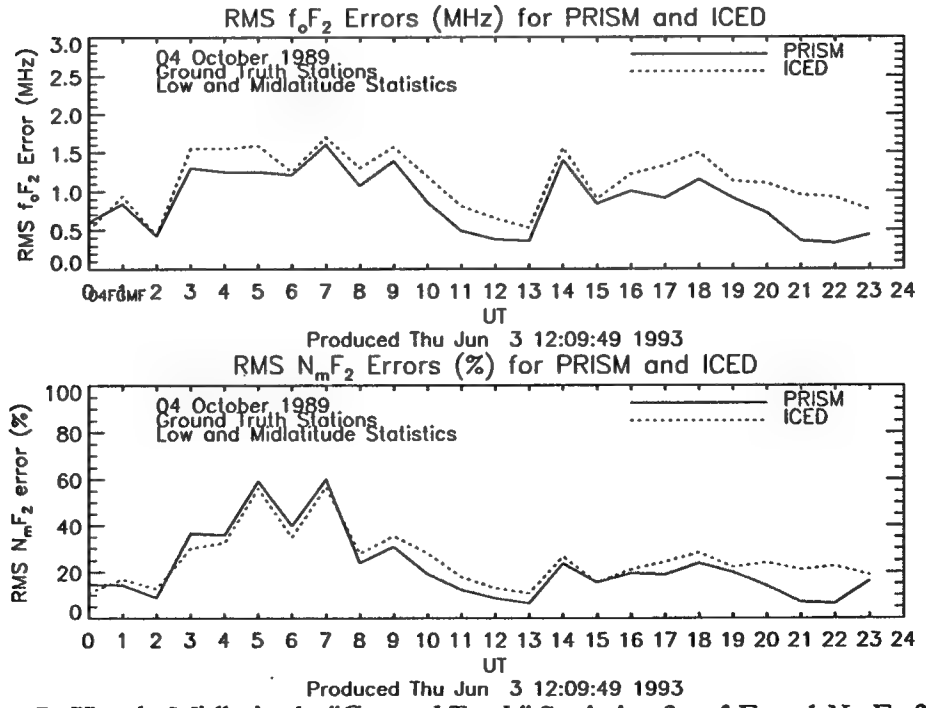

Figure 5. Hourly Midlatitude *"Ground Truth"* Statistics for f_oF_2 and N_mF_2 for 4 October 1989.

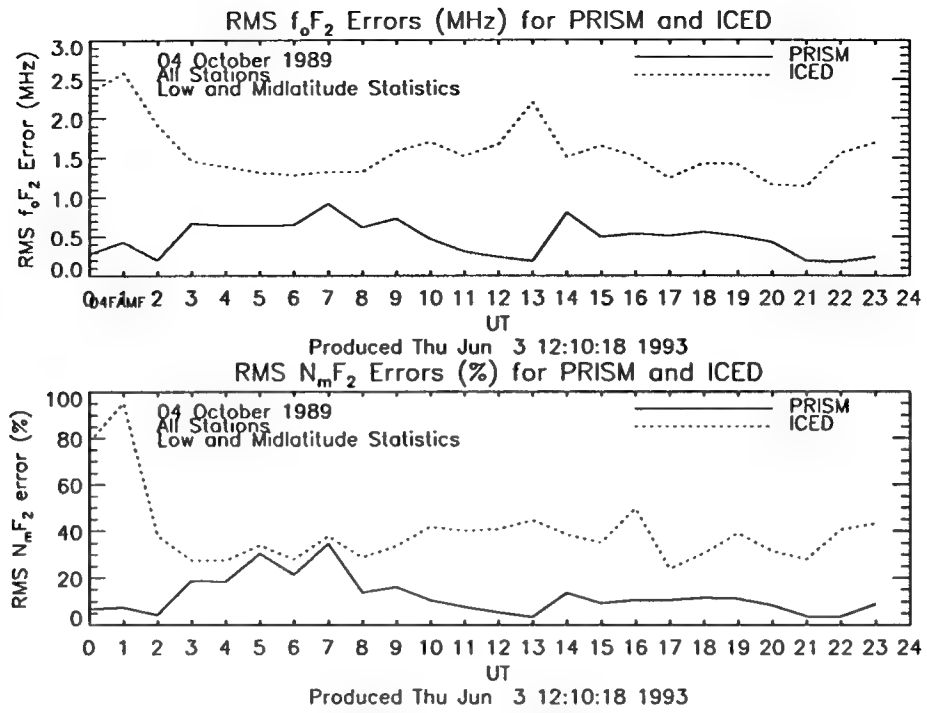

Figure 6. Hourly Midlatitude Statistics for *All Stations* for f_oF_2 and N_mF_2.

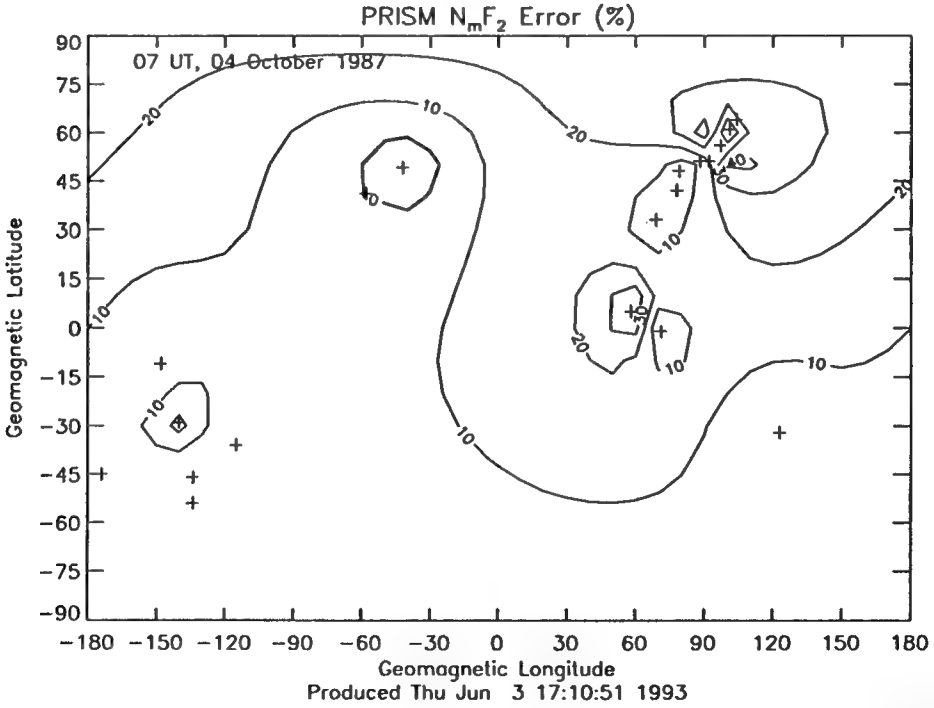

Figure 7. Contours of PRISM N_mF_2 Error (%) for 0700 UT on 4 October 1989.

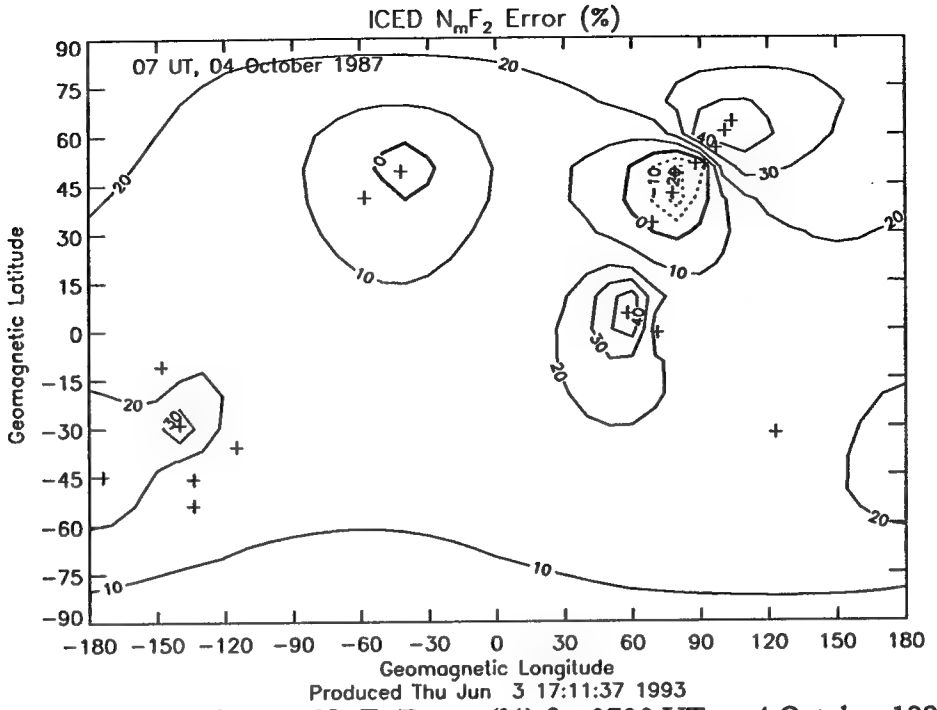

Figure 8. Contours of ICED N_mF_2 Errors (%) for 0700 UT on 4 October 1989.

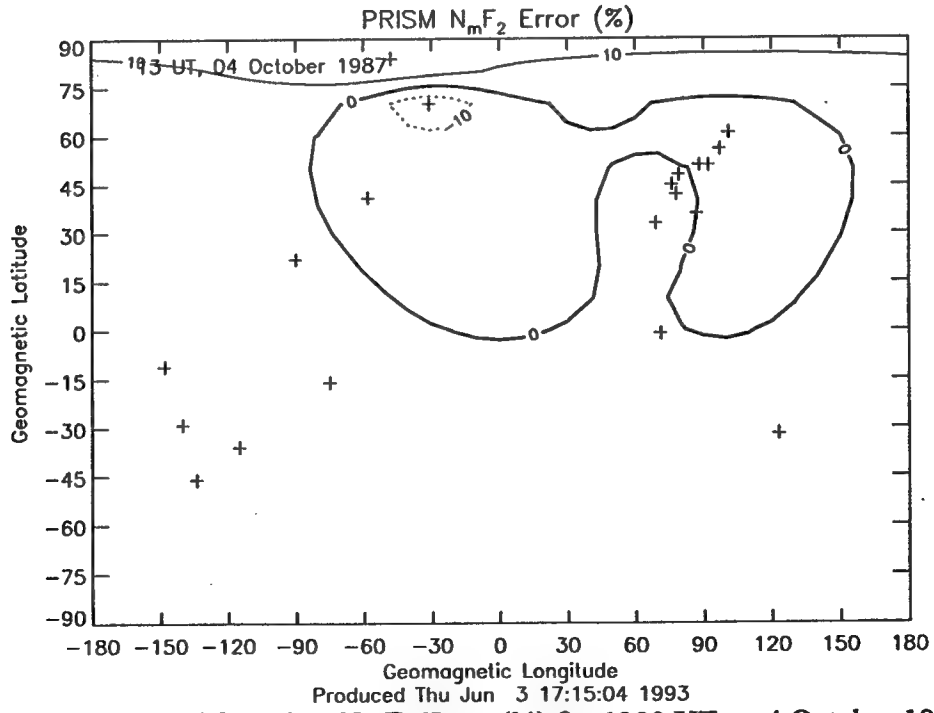

Figure 9. Contours of PRISM N_mF_2 Error (%) for 1300 UT on 4 October 1989.

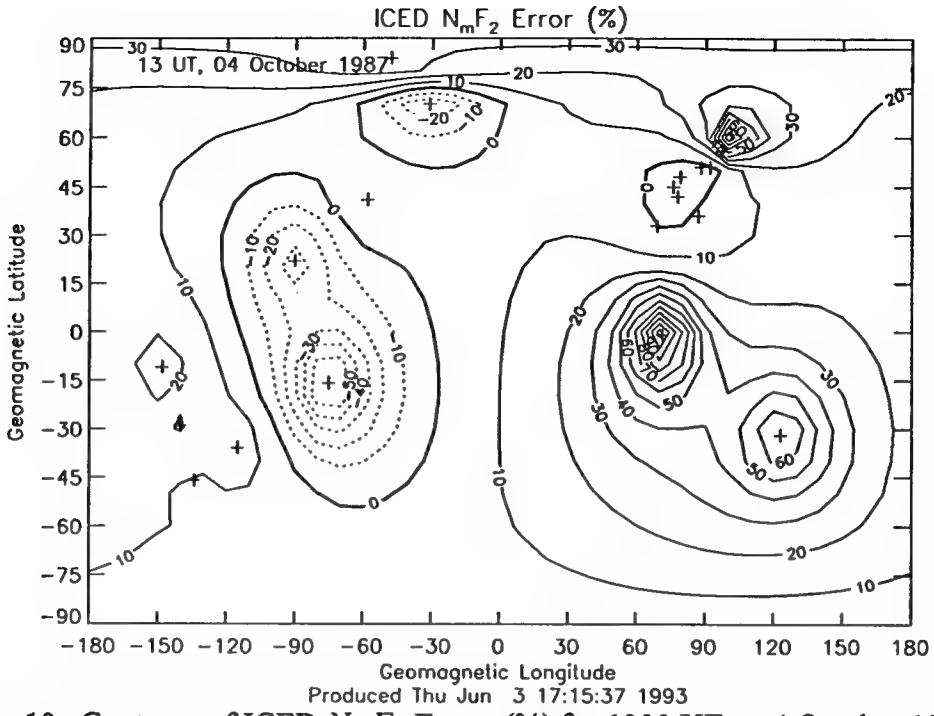

Figure 10. Contours of ICED N_mF_2 Errors (%) for 1300 UT on 4 October 1989.

5.2 h_mF_2 Validation

As we discussed in the section on data acquisition, we did not have very much digital ionosonde data available. Since true height analysis is generally not available from analog ionosondes, this means that we did not have much height information to use to drive PRISM. That is why we extended our original validation period of 2-6 October to include 9 October. On that day, the five Digisondes in the U. Mass. Lowell chain were all operating continuously and returning true height data at least once per hour. So we selected four of the five Digisondes as drivers and used the remaining one for "ground truth."

The h_mF_2 statistics were generated at the same time as the f_oF_2 and N_mF2 statistics, of course. They are summarized in Table 16. As with f_oF_2 and N_mF2, PRISM accurately reproduces the low and midlatitude driver data, but in this case, PRISM also outperforms ICED at the "ground truth" site. However, since there is only a single ground truth site for h_mF_2, we cannot guarantee this will be the case at any distance from driver data.

Table 16. Global and Midlatitude Statistics for h_mF_2 errors on 9 October 1989.

Station Type	Station Hours	RMS Errors (km) ICED	PRISM	PRISM "Improvement"
Global Statistics				
driver	93	27	24	11%
other	24	20	13	35%
all	117	25	22	12%
Midlatitude Statistics				
driver	71	27	0	99%
other	24	20	13	36%
all	95	25	6	75%

5.3 Topside Validation

Because the ISR data do not extend above 600 km, we have no "ground truth" for PRISM's topside specification. Consequently, we cannot actually validate PRISM's topside algorithm beyond the simulation using ISR data presented in the section **PRISM F Region Adjustments**. However, we have made several runs using SSIES data from DMSP F8 and F9 Satellites to demonstrate that PRISM can ingest and use this data. Unfortunately, two important components of SSIES were not functioning during this time period: the Retarding Potential Analyzer and the Langmuir Probe. Thus, the only in situ data available was the total ion density (= electron density) and the ion drift speed. Nevertheless, we present here the results of one run for 1400 UT on 4 October 1989 when DMSP F9 passed nearly overhead of the Arecibo (Puerto Rico) ISR.

We used 30 second averages of the SSIES ion density from the Scintillation Meter. Since the satellite moves at about 6½ km/sec, this gives us a spatial resolution of about 200 km, more than adequate for the topside adjustment. (We use 5-second averages for the ion drift velocity, allowing us to locate the convection boundary with a resolution of about 35 km.) The closest datum to Arecibo came at 1355:44 UT at which time the satellite was at 18.50^{o}N, 291.41^{o}E (geographic). This is about 200 km away from the site and 4¼ minutes before the ionospheric specification. The ISR data have been binned and averaged, however, and the central time of the averaged data is actually 1330 UT. So the ionospheric specification and the SSIES data are being compared to ISR data from one-half hour earlier.

Figure 7 shows the EDP's produced by ICED and PRISM compared to the ISR data. The curve marked "PRISM u" is the profile produced by PRISM using only $F_{10.7}$, SSN_{eff}, and K_p as input. The curve marked "PRISM i & t" is the profile produced when ionosonde and TEC data are used. And the solid curve is the profile produced when SSIES data is also used. Because there was no ionosonde near the ISR site, PRISM does not reproduce the peak. PRISM's error is comparable to ICED's. (Note again the large difference between the actual value and that predicted by climatology.) PRISM does reproduce fairly well the SSIES density of 1.04×10^{5} cm^{-3} at 825 km.

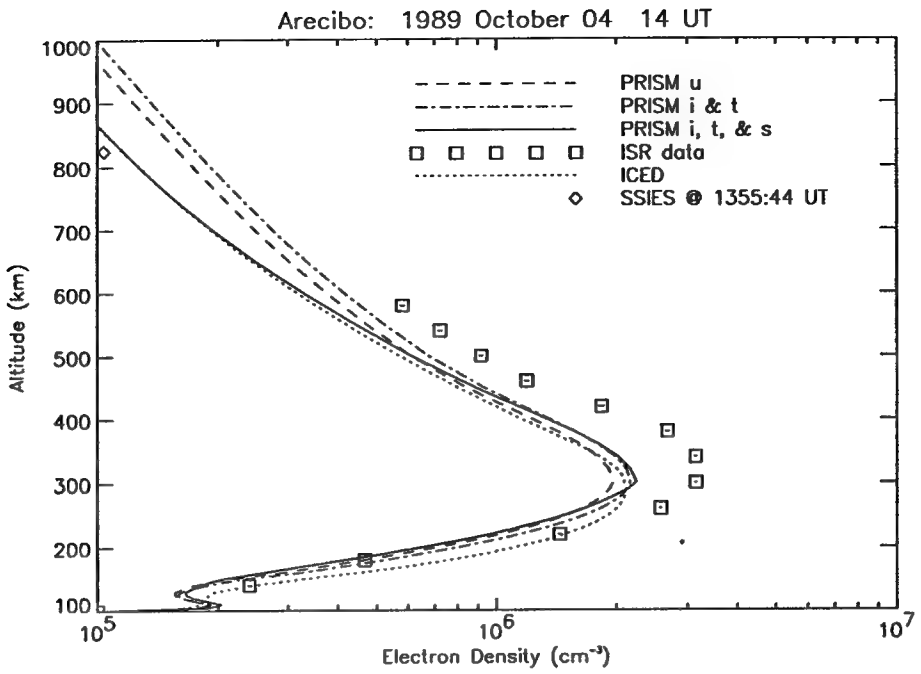

Figure 11. PRISM, ICED, and ISR Electron Density Profiles for 1400 UT on 4 October 1989. See text for explanation of PRISM profiles.

Note that extrapolating the ISR EDP to 840 km does not appear to agree with the SSIES value. There are several possibilities for this disagreement:

1. One or both of the experiments is in error.
2. The difference is due to the separation in time and space of the two measurements.
3. We know that the elevation angle of the ISR data was "above 70^{o}," but we don't know its exact value, and we don't know the azimuth. Therefore, the distance between the ISR observation (extrapolated to 840 km) and the DMSP location may be much larger than the nominal 200 km.
4. The topside ionosphere may have more structure than a simple extrapolation would allow.

Nevertheless, this points up the difficulties of (1) specifying the ionosphere in real time, and (2) testing or validating any specification or forecast model.

6. TEC Validation

As was the case for h_mF_2 validation, we did not have a great deal of TEC data. Consequently, our validation has been rather limited. As described in the **Data Acquisition** section, we had four polarimeters forming a chain along the east coast of North America. We used three of these as drivers and the fourth as ground truth. These instruments were very reliable and reported TEC throughout the month. They were used in all the runs for 2-6 October, so the TEC statistics were generated at the same time as the f_oF_2 and N_mF_2 statistics. The results for each day and for all 5 days together are presented in Table 17. It is interesting to note that ICED did consistently better at the "ground truth" station than at the three "driver" stations. (Since the "driver" stations did not contribute to either of the inputs to ICED, they were not drivers of ICED, only of PRISM.) The conclusions are the same as for the F layer parameters. PRISM provides a significant improvement where there is data, but is no better than climatology where data is lacking.

Table 17. Midlatitude Statistics for TEC errors.

	Station	Station	RMS Error (TEC units)		RMS Error (%)		PRISM
Date	Type	Hours	ICED	PRISM	ICED	PRISM	"Improvement"
2 Oct	Driver	72	8.5	0.3	44%	3%	93%
	Other	24	4.1	4.9	18%	15%	19%
	All	96	7.6	2.5	39%	8%	80%
3 Oct	Driver	72	8.3	0.4	43%	4%	92%
	Other	24	3.4	4.6	16%	14%	18%
	All	96	7.4	2.3	38%	7%	81%
4 Oct	Driver	72	7.6	0.2	26%	1%	96%
	Other	24	2.4	6.4	8%	14%	-83%
	All	96	6.7	3.2	23%	7%	69%
5 Oct	Driver	72	7.3	0.2	29%	1%	96%
	Other	24	3.6	7.3	12%	17%	-38%
	All	96	6.5	3.7	26%	8%	67%
6 Oct	Driver	72	8.7	0.1	29%	1%	98%
	Other	24	5.0	6.5	10%	15%	-56%
	All	96	8.0	3.3	26%	8%	70%
2-6	Driver	72	8.1	0.3	35%	2%	94%
Oct	Other	24	3.7	6.3	12%	15%	-25%
	All	96	7.3	3.0	31%	8%	75%

7. High Latitude Validation

There was insufficient high latitude data to perform a meaningful validation. Consequently, we present here some graphical PRISM output to demonstrate that PRISM can ingest high latitude data, including SSJ/4 data, and use it to refine its ionospheric specification. In Figures 12 and 13 we show contour plots of f_oF_2 and f_oE for 1400 UT on 4 October 1989, the same case presented in Figure 11 (demonstrating the use of SSIES data). In Figure 14, we also show a plot of the boundaries determined from the SSIES and SSJ/4 data. The plotted boundaries are more structured than the actual PRISM boundaries due to the coarseness of the grid (2° in latitude, 5° in longitude) and the method used to plot them. A numerical code was assigned by PRISM to each grid point indicating its region: midlatitude, trough, auroral oval, polar cap. The boundaries were then determined by the contouring software. The outermost boundary is the equatorward edge of the trough. The middle boundary is the equatorward edge of the auroral oval. The innermost boundary is the equatorward boundary of the polar cap.

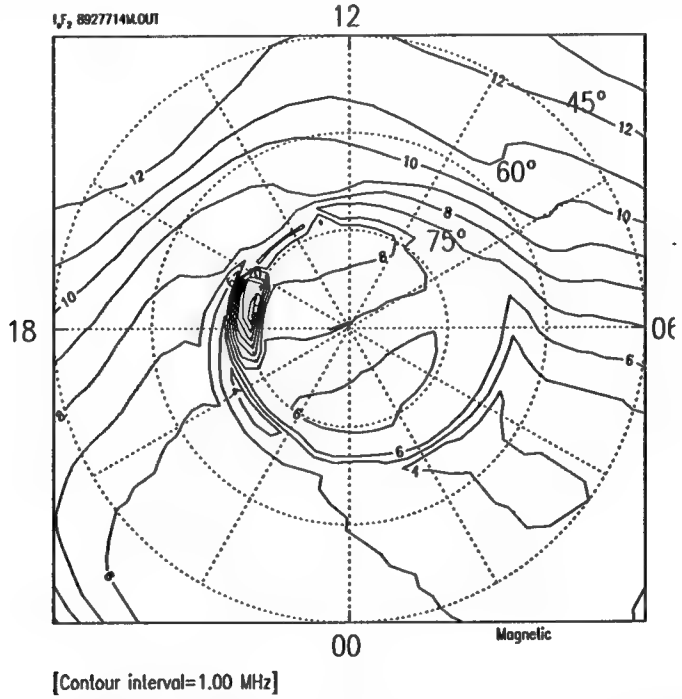

Figure 12. Contours of PRISM f_oF_2 for 1400 UT on 4 October 1989, demonstrating the use of SSIES and SSJ/4 data.

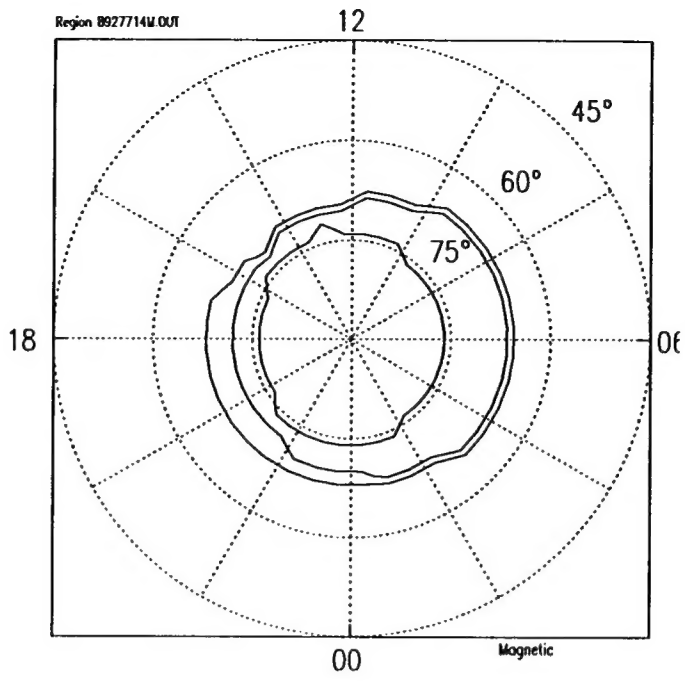

Figure 13. Contours of PRISM f_oE for 1400 UT on 4 October 1989, demonstrating the use of SSIES and SSJ/4 data.

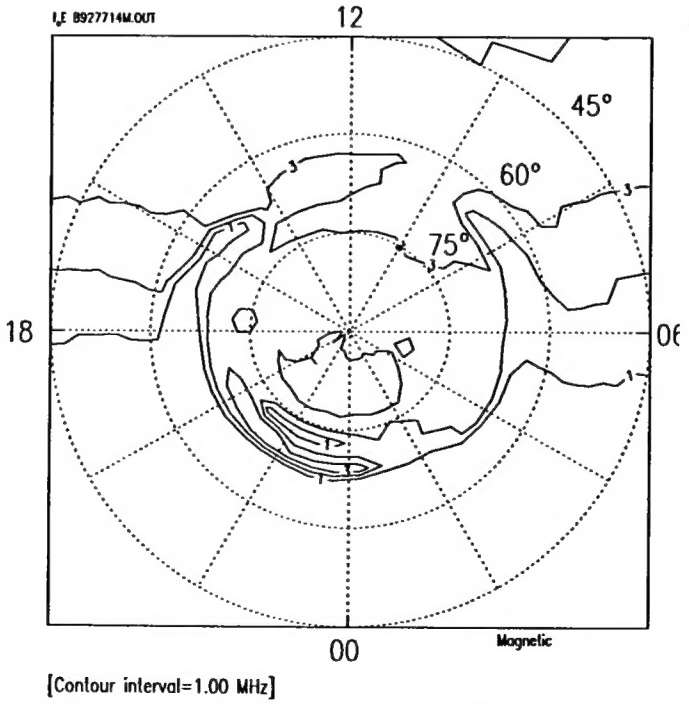

Figure 14. High latitude boundaries at 1400 UT on 4 October 1989 as determined by PRISM using SSIES and SSJ/4 data. See text for explanation.

Section 8: Conclusions

We have demonstrated that PRISM is capable of ingesting data from a wide variety of sources and that it can use that data to significantly improve its ionospheric specification over climatological models. In particular, while ICED ingests ionosonde data as a single number (effective sunspot number), PRISM ingests all of the ionosonde data as well as TEC data and adjusts its profiles to reproduce that data. While ICED's profiles are fixed on the basis of two input parameters (SSN_{eff} and K_p), PRISM's profiles are adjusted on the basis of ionosonde data, TEC data, in situ plasma data, and particle precipitation data. At the sites where data are taken PRISM's improvement over ICED approaches 100%. Because the correlation length of the ionosphere is only about 1000 km (or less), the improvement becomes small in regions well away from the data sources. However, as the Air Weather Service adds new sources of data (TISS, UV imaging, etc.) PRISM will be able to ingest it and increase the area over which its specifications are more accurate than climatology.

UV imaging has the potential to greatly increase the accuracy of AFSFC's ionospheric specifications. Because the EDP information derived from the UV images "looks" like ionosonde data to PRISM, little or no modification will be required to allow PRISM to ingest and use this data. DMSP UV image data and EDP information derived from it should be available before the end of the decade.

Although it now appears that only five TISS receivers will be placed in operation, each receiver will provide several measurements of TEC in different directions. They will greatly improve PRISM's ionospheric specification for the entire region surrounding each TISS site and, therefore, greatly improve AFSFC's support for Air Force operations at those sites. In addition, there is a large network of dual frequency GPS receivers whose data is coordinated by the Jet Propulsion Laboratory (JPL) in Pasadena. Although this data is not currently available in near real time, it is available within 24 hours, which could be useful for post event analysis. If the data can be made available in real time, it would have a significant and positive impact on the accuracy of PRISM's ionospheric specification, particularly in areas not represented by DISS sites. Again, no modification of PRISM is required for it to utilize either TISS or other TEC data.

Finally, we strongly recommend that PRISM undergo further validation, preferably on a regular and continuing basis, once it is operational at AFSFC. This validation should involve personnel from AFSFC, ETAC, PL/GPIM, and CPI. "Validation Days" should be selected in

advance so that both the real-time input data and PRISM output can be archived. Data from independent sources (NGDC, university Digisondes) should be collected by PL/GPIM for comparison to the archived PRISM output. This activity should be over and above any "problem resolution" or "bug report" activity carried out as a result of operational problems with PRISM. It will be useful both for quantifying PRISM 1.2 performance and for identifying areas for possible future improvement.

9. References

Geomagnetic Indices Bulletin, published monthly by National Geophysical Data Center (E/GC2), 325 Broadway, Boulder, CO 80303.

Hardy, D. A., L. K. Schmitt, M. S. Gussenhoven, F. J. Marshall, H. C. Yeh, T. L. Schumaker, A. Huber, and J. Pantazis, *Precipitating Electron and Ion Detectors (SSJ/4) for the Block 5D/Flights 6-10 DMSP Satellites: Calibration and Data Presentation*, AFGL-TR-84-0317, Phillips Laboratory, Hanscom AFB, Massachusetts, 1984. **ADA157080**

Reinisch, B. W., and Huang Xueqin, Automatic calculation of electron density profiles from digital ionograms, 3. Processing of bottomside ionograms, *Radio Sci.*, **18**, 477-492, 1983.

Solar Indices Bulletin, published monthly by National Geophysical Data Center (E/GC2), 325 Broadway, Boulder, CO 80303.